NISTIR 4994

# Simulating the Effect of Beamed Ceilings on Smoke Flow, Part I. Comparison of Numerical and Experimental Results

Glenn P. Forney
William D. Davis
John H. Klote

United States Department of Commerce
Technology Administration
National Institute of Standards and Technology

# NISTIR 4994

# Simulating the Effect of Beamed Ceilings on Smoke Flow, Part I. Comparison of Numerical and Experimental Results

Glenn P. Forney
William D. Davis
John H. Klote
Building and Fire Research Laboratory
Gaithersburg, MD 20899

December 1992


**U.S. Department of Commerce**
**Barbara** Hackman Franklin, ***Secretary***
Technology Administration
Robert M. White, ***Under Secretary for Technology***
National Institute of Standards and Technology
John **W.** Lyons, ***Director***

# Contents

# List of Figures



# List of Tables

# Simulating the Effect of Beamed Ceilings on Smoke Flow, Part I. Comparison of Numerical and Experimental Results

Glenn P. Forney William D. Davis John H. Klote

**Abstract**

The flow of smoke under beamed ceilings is simulated using a field model. This work was performed in order to confirm that fire detector response can be evaluated using computational data obtained from numerical simulations as well as laboratory data obtained from experiments. The field model is verified for this application by showing that its temperature predictions match experimental results obtained earlier by Heskestad and Delichatsios. Line plots are presented which show that the numerical and experimental temperature measurements are in good agreement. Contour plots are also presented that show the temperature distribution in the channels formed by the ceiling beams. Finally some preliminary results involving the effect of beam depth on smoke flow are presented.

## 1 Introduction

Experiments were performed by Heskestad and Delichatsios in the late seventies in order to evaluate the response of fire detectors under flat ceilings[1, 2] and beamed ceilings[3, 4]. Quoting from [3],

> "The major objective of this work was to generate graphical and tabular presentations of the environmental data in both physical forms and "reduced" forms, the latter allowing extrapolation of the data to arbitrary combination of ceiling heights and fire-growth rates. **A** second objective was to confirm previously established methods of predicting the response of fire detectors from the environmental data and subsequently to determine optimum spacing of fire detectors under large beamed ceilings."

These goals can also be realized by using numerical simulations to produce the data from which graphical and tabular presentations are derived. This report documents

the first step in this process, a comparison of numerical and experimental results. Ultimately, the goal of this work is to provide a basis for sound recommendations for modifications to NFPA 13 and 72E.

Six beam configurations were investigated experimentally [3, 4]. Three configurations consisted of beams with dimensions 0.305 m (1.00 ft) by 0.152 m (.5 foot) with 0.61, 1.22 and 1.83 m (2, 4 and 6 ft) center to center spacing. The other three configurations consisted of beams with dimensions 0.61 m (2. ft) by 0.305 m (1 ft) with 1.22, 2.44 and 3.66 m (4, 8 and 12 ft) center to center spacing. Each of these six configurations consisted of a solid floor, beamed ceiling and open walls. Three experiments were performed for each configuration. An additional three experiments were performed with draft curtains in addition to the beams.

A short beam spaced experiment, experiment 4, and a medium beam spaced experiment, experiment 16, were chosen for the comparisons in this report. The large beam spaced experiments, experiments 19, 20 and 21, required more grids to simulate two channels than the short and medium case which would have required more computer time. Experiment 4 consisted of ceiling beams spaced 1.22 m (4 ft) apart with a depth of 0.305 m (1 ft). Experiment 16 consisted of ceiling beams spaced 2.44 m (8 ft) apart with a depth of 0.61 m (2 ft). Numerical results predicted by a field model are shown to be in substantial agreement for these two experiments. Wood cribs with measured heat release rates were used as the fire source.

# 2 Simulating the Smoke Flow

## 2.1 Model

Release 2.3.2 of FLOW3D was used to perform the numerical simulations described in this report[5]. This field model has been previously applied to model the fire at the King's Cross underground station [6]. These numerical results were subsequently verified with 1/3 scale fire experiments[?]. The field model has been successfully applied to two well instrumented full scale room experiments[8]. It was also used to predict the interaction of wind, a fence and a fire near an outdoor fire fighting facility[9].

The field model solves the three dimensional form of the equations for conservation of mass, momentum, and energy. The required physical parameters for these equations include fluid density, pressure, specific heat at constant pressure, acceleration of gravity, thermal conductivity and molecular viscosity. It was assumed that the fluid was air and that it was fully compressible. Turbulence was modeled using the $k - \varepsilon$ model[5, 10]. The floor, ceiling and beams were assumed to be adiabatic. Radiation effects were not included in the calculation except that only a fraction of

the heat release rate was assumed to contribute to convective heating of the smoke and air. The rest of the heat was considered to be radiated away.

**A** rectangular, non-uniform grid was used to model each experiment. An upwind differencing scheme was used to model the advection terms. The equations were advanced in time using a fully implicit backward difference procedure.

The grid was set up so that the fire was at the origin (see Figure 1). Six boundary conditions are required, two for the floor and ceiling and one each for the four walls. The floor and beamed ceiling were specified to be solid. **A** no-slip boundary condition was assumed along these solid boundaries. Open boundaries were specified for the two walls away from the fire. Symmetry planes were used for the two boundaries near the fire. The symmetry boundary condition specifies that flow will be tangent to the boundary so that no flow will occur across the boundary. The two symmetry planes split the experimental region into four regions. It is also assumed that the fire contributed equally to each of these four regions.

## 2.2 Experiment

The fire source consisted of a wooden crib constructed with 15 layers, **14** sticks per layer of clear sugar pine. Each stick had dimensions of 0.159 m x 0.159 m x 0.762 m (5/8 in x 5/8 in x 30 in) Heskestad and Delichatsios used the following procedure in [3] to determine the energy release rate of the fire. Cumulative weight loss was measured for the burning crib for each experiment. This data was then converted to average burning rates using the experimentally determined value of heat of combustion for clear sugar pine of 20.9 MJ/kg (9000 Btu/lb). It was noted in [4] that a plot of the square root of the energy release data versus time was approximately linear. Therefore the burning rates were used to curve fit the expression

$$\sqrt{Q(t)} = \sqrt{\alpha}(t - t_0)$$

or equivalently

$$Q(t) = \alpha(t - t_0)^2 \ .$$

where $Q(t)$ is the heat release rate at time $t$, $a$ is a proportionality constant and $t_0$ is the time origin. For experiment 4, $a$ was computed to be **13.47** $W/s^2$ (0.01277 $Btu/s^3$). Similarly, for experiment 16, $\alpha$ was computed to be 12.8 $W/s^2$ (0.01211 $Btu/s^3$).

Radiation losses from the fire were estimated to be ***35*** per cent ($\chi_r = 0.35$). Experiment 16 was simulated using $\chi_r$ values of 0.25, 0.35 and 0.45 . It was found that $\chi_r = \mathbf{0.35}$ gave the best agreement between the numerics and experiment. The

numerical time origin, $t_0$ was set to zero. The heat release rate used to simulate experiments 4 and 16 was then

$$Q(t) = \frac{(1 - \chi_r)\alpha}{4} t^2$$

where $\chi_r = 0.35$ and $\alpha = 13.47 \mathrm{W/s^2}$ for experiment 4 and $\alpha = 12.8 \mathrm{W/s^2}$ for experiment 16. The virtual time origins, $t_0$, found in Table II of [4] were used to specify the starting time of the experiment for the purpose of numerical-experimental comparisons.

# 3 Comparison of Numerical and Experimental Results

Numerical field modeling can effectively complement laboratory experiments as long as the two approaches give consistent results in a comparable time. The next two sub-sections present results that show that the two approaches are in good agreement. A typical 5 minute simulation took approximately 48 hours of computer time on a Silicon Graphics 4D35 work station. For simple grids, it usually takes a few hours to set up a case. Several runs are required to insure that a case is set up correctly. The time for setting up and running a field model is shorter than the time required to set up and perform laboratory experiments. This time will be reduced by a factor of 2.5 to 4 as faster computers soon become available. Therefore field modeling is a good approach for solving these types of problems.

## 3.1 Experiment 4 - 0.305 m (1 ft) Beams Spaced 1.22 m (4 ft) Apart

Figure 1 shows a schematic of the top view for the setup for experiment 4. This figure corresponds to Figure 1b in [4]. The numbers denote temperature sensor locations. These sensors are located 0.152 m (0.5 ft) below the ceiling. The $x$ and $y$ locations are detailed in Table 1. The distances are measured with respect to the fire. The fire source, a wood crib, was located at position 0.

The portion of the experiment simulated using the field model is outlined with the small interior rectangle in Figure 1. The simulated region includes four flow channels. A channel refers to the space near the ceiling between adjacent beams. The beams tend to isolate or channel the smoke flow. Therefore, the temperature tends to drop more rapidly towards ambient across channels than within a channel. Because of this, four channels are sufficient to simulate the main features of the experiment. The

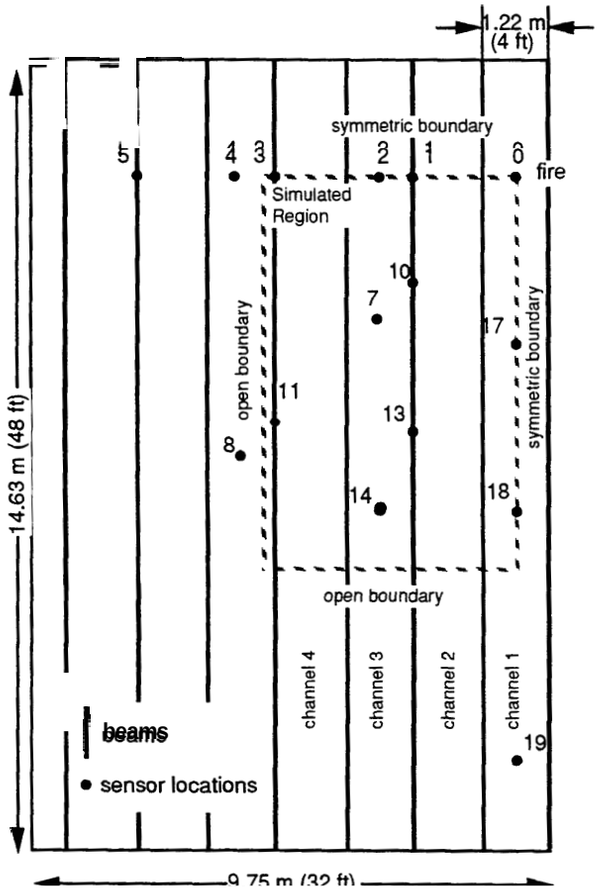


Figure 1: Physical Configuration for Experiment 4

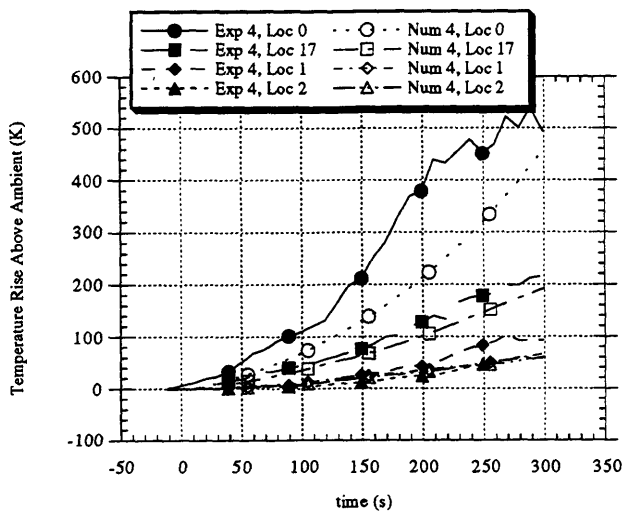


Figure 2: Comparison of Numerical and Experimental Temperatures at Sensor Locations 0, 17, 1 and 2 for Experiment **4**

vertical dimension of grids near the floor are 0.61 m (2.0 ft) while grids near the ceiling have a vertical dimension of **0.305** m (1. ft). The horizontal grid dimensions are for the most part 0.305 x 0.305 m (1. ft x 1. ft). The grids are smaller near the beams to better resolve the flow and to simulate the correct beam spacing.

Figure **2** shows **a** comparison between temperatures measured in experiment 4 and temperatures calculated using the field model at locations 0, 17, 1 and 2. Temperature comparisons were made for all locations within the shaded rectangle except for locations 3 and 11. These locations are under the beam in the fourth channel and had a temperature rise of only about 10 K (18 °F) at 300 seconds. Temperature comparisons are shown in Figure **2** for location 0 (above the fire), location 17 (in first channel), location 1 (under the beam separating the second and third channel) and location 2 (in the third channel). The temperature comparisons for other locations (18, 10, 13, 7 and **14)** are similar to those shown in Figure 2.

The field model calculates the temperatures at the center of each grid cell. The temperature at the instrument locations were calculated by linearly interpolating this data using the B3INK/B3VAL software [11] which implements tensor product B-spline interpolation algorithms [12, 13].

The agreement between numerical and experimental temperature measurement directly over the fire is not good. This is surprising in view of the good matches that were obtained at all other locations for both experiment 4 and experiment 16. The temperature gradient (changes in temperature over short distances near the fire) is

Table 1: Instrument Locations Used in the Experiment 4 Comparison

| Instrument Location | X (m) | Y (m) |
|---|---|---|
| 0 | 0.00 | 0.00 |
| 1 | 1.83 | 0.00 |
| 2 | 2.44 | 0.00 |
| 7 | 2.44 | 2.44 |
| 10 | 1.83 | 1.83 |
| 13 | 1.83 | 4.42 |
| 14 | 2.44 | 5.88 |
| 17 | 0.00 | 3.05 |
| 18 | 0.00 | 6.10 |

large near grid cells containing the fire plume. Both experimental and numerical temperature measurement will therefore be more sensitive to the measurement locations when near the fire. Temperature comparisons at other locations, however, as seen in the plot are quite good. The field model successfully predicts quantitatively the temperature rise with time and the temperature drop off that occurs going from the first channel containing the fire to the third channel. The experimental data used for the comparison was obtained from [3].

Figures **3,** 4, 5 show how the hot gasses generated by the fire plume are channeled by the beams. The fire in Figure **3** is located in the upper right corner. The fire in Figures 4 and 5 is located in the lower right corner. The contours represent the temperature rise above ambient. The contours in Figure 3 lie in a plane parallel to the ceiling located just below the beams. This figure shows the temperature rise that occurs between the edge of the plot and the first beam. The temperature rise in the second channel is 90 K at the bottom of the plot near the fire and 60 K at the top away from the fire. The temperature rise in the third channel is 30 K. The contours in Figure 4 lie in a vertical plane perpendicular to the beams. The three "notches" at the top of the plot indicate the location of the three beams. The temperature rise is confined to the first channel. The contours in Figure 5 lie in a vertical plane parallel to the beams. The plane is in the middle of the first channel. This plot again shows the temperature rise occurring in the first channel. Similarly plots in other planes parallel to this one do not contain the high temperatures that this plot does. Similar contour plots with shorter beam depths show as expected, smoke flow that is less channeled.

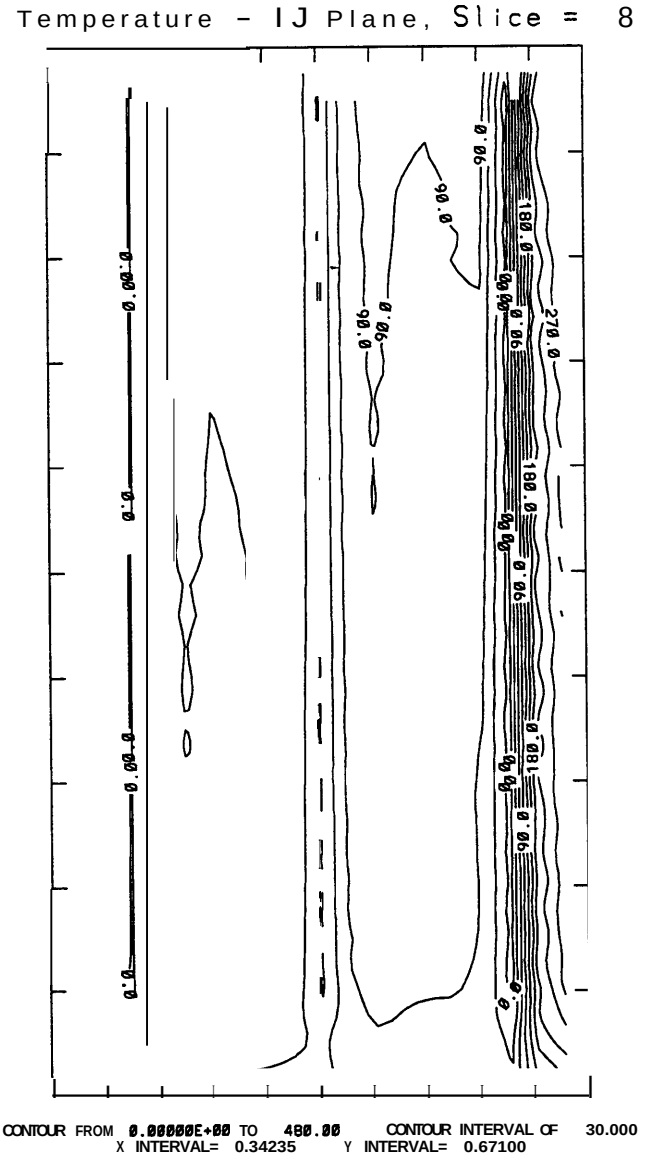


Figure **3:** Numerical Temperature Rise Contours (K) for Experiment **4** - Slice 8, **A** Plane Parallel to the Floor Just Below the Ceiling

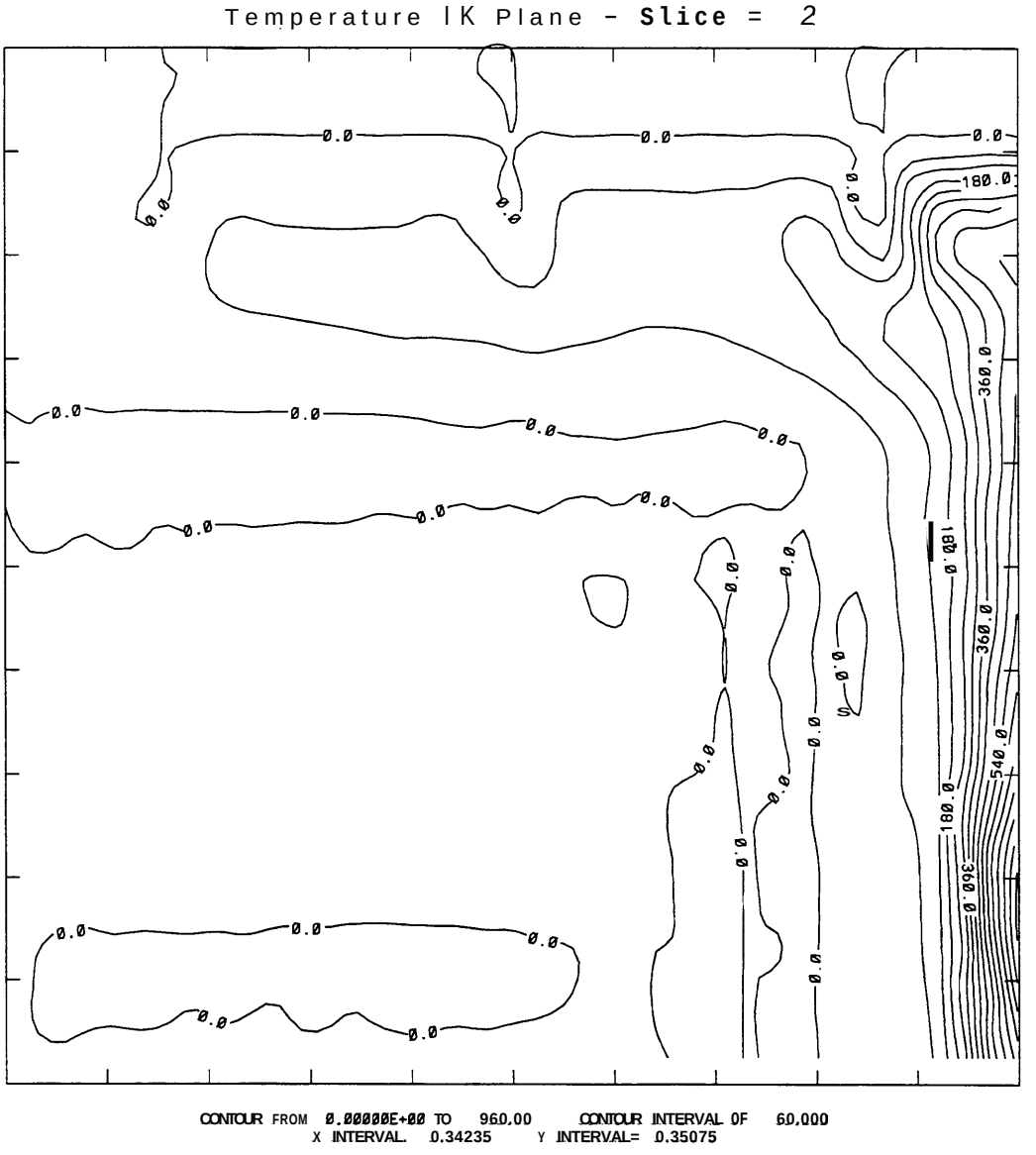


Figure 4: Numerical Temperature Rise Contours (K) for Experiment 4 - Slice 2, **A** Vertical Plane Containing the Fire, Perpendicular to the Beams

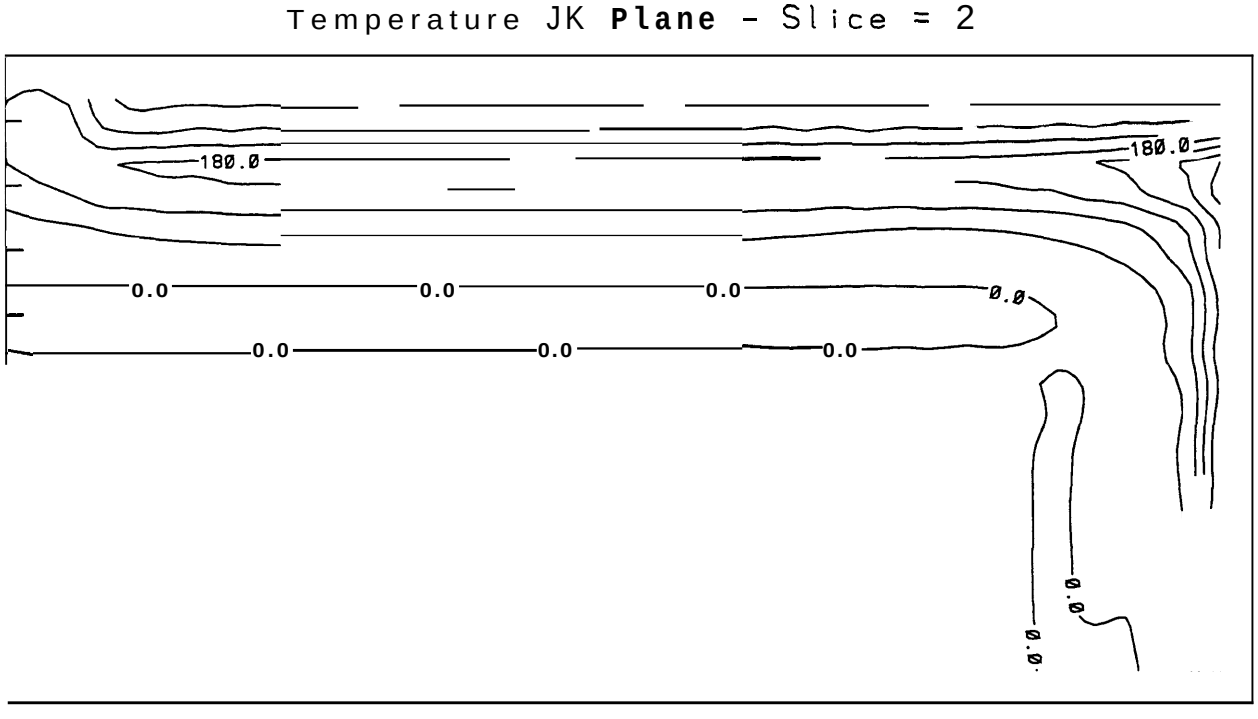


Figure *5:* Numerical Temperature Rise Contours (K) **for** Experiment **4** - Slice **2, A** Vertical Plane Parallel to the Beams

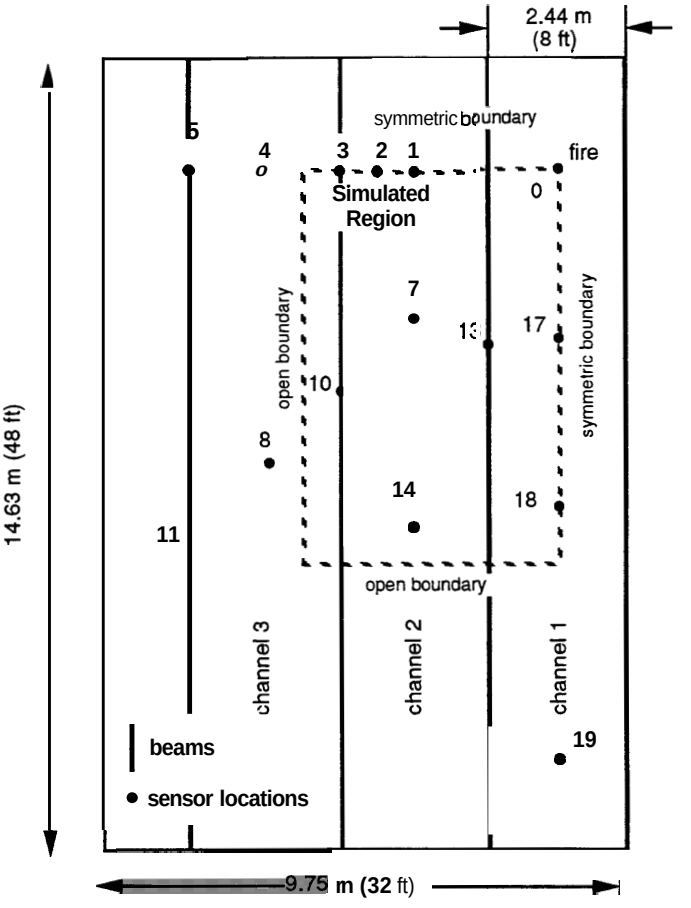


Figure 6: Physical Configuration for Experiment 16

## 3.2 Experiment 16 - 0.61 m (2.0 ft) Beams Spaced 2.44 m (8 ft) Apart

Figure 6, similar to Figure 1, shows a schematic of the top view of the experimental configuration for experiment 16. The essential difference between these two figures is that the beams are spaced 2.44 m (8 ft) apart rather than 1.22 (4 ft) apart. Due to the wider spacing, the temperature comparisons are made in adjacent channels rather than every third channel. Again, the numbers denote the temperature sensor locations. The sensors are located 0.152 m (0.5 ft) below the ceiling (or beam) and the fire source is located at position 0. The thick solid line denotes the beams and the dashed inner rectangle indicates the portion of the physical experiment that was simulated numerically. Temperature comparisons made at location 0 (over the fire),

Table 2: Instrument Locations Used in the Experiment 16 Comparison

| Instrument Location | X (m) | Y (m) |
|---|---|---|
| 0 | 0.00 | 0.00 |
| 1 | 1.83 | 0.00 |
| 7 | 1.83 | 2.44 |
| 14 | 1.83 | 5.88 |
| 17 | 0.00 | 3.05 |
| 18 | 0.00 | 6.10 |

17 (in the first channel near the fire) and 1 (in the second channel) are shown in Figure 7. Data for the comparison was obtained from [3]. Comparisons were also made at locations 18, 7, 14 and 2 with comparable results. The temperature rise at location 3 and 10 was only 7.2 K (13.0 °F), 5.0 K (9.0 °F) respectively. The physical locations of these instruments are recorded in Table 2. As seen in the plot, the numerical and experimental temperature measurements compare quite well for each sensor location. Again, the field model predicts quantitatively both the temperature rise with time and the temperature fall off that occurs in adjacent channels including the sensors directly over the fire.

Figures 8, 9 and 10 show temperature contour plots for three orientations in Experiment 16. The fire is located in the upper right corner of Figure 8 and the lower right corner of Figures 9 and 10. The smoke flow is contained within the beam channels more in this experiment than in Experiment **4** since the beams depths are 0.61 m (two ft) instead of 0.305 m (one ft). Figure 8 shows a temperature contour plot for a plane near the ceiling parallel to the floor. Figure 9 shows a temperature contour plot for a plane containing the fire that is perpendicular to both the floor and the beams. Figure 10 shows a temperature contour plot for a plane containing the fire that is perpendicular to the floor but parallel to the beams. A comparison of these three contour plots with the corresponding plots for experiment 4 (Figures 3, 4 and **5)** shows the effect of the deeper beams and wider channels. The temperature drop off between adjacent channels is greater. In experiment 16, the temperature rise in the adjacent channel is 30 K (Figure 8) while in experiment 4, the temperature rise is 90 K (Figure 3).

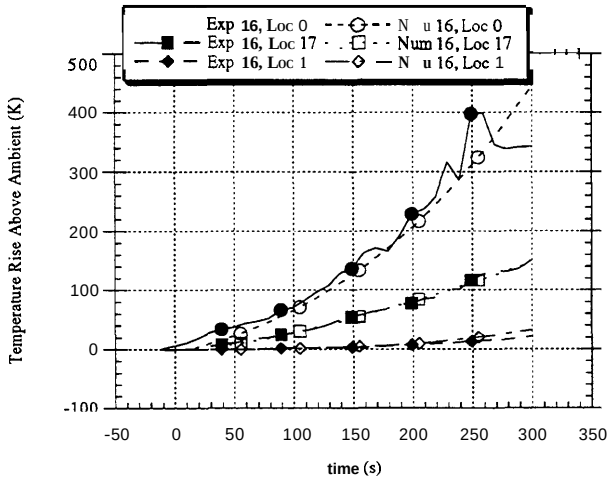


Figure 7: Comparison of Numerical and Experimental Temperatures at Sensor Locations 0, 17 and 1 for Experiment 16

# 4 A Preliminary Examination Of Other Beam Configurations

The next step in this work is to perform a variety of numerical experiments for configurations not given in [3] in order to study the effects of beam depths, beam spacing, ceiling heights and fire size on the distribution of heat and smoke near the ceiling. Data obtained from these numerical results will be reduced to contour plots (similar to those shown earlier) of heat and smoke distribution.

**As** a start in this direction, two numerical experiments were performed which varied the beam depth of experiment **4,** in order to investigate the above effects. Recall that the beam depth for experiment 4 was **0.305** m. The beam depths for the two additional numerical experiments were 0.152 m and 0.076 m respectively. Figures 11 and 12 show the temperature rise above ambient found in the .152 m and 0.076 m beam depth configurations. The beams in both configurations are spaced 1.22 m (4 ft) apart. Due to the shorter beam depth more smoke flows into the second and third channels. This effect is more pronounced for the shorter beam depth case as illustrated in Figure 12. The fire is located in the upper right corner of the contour plot.

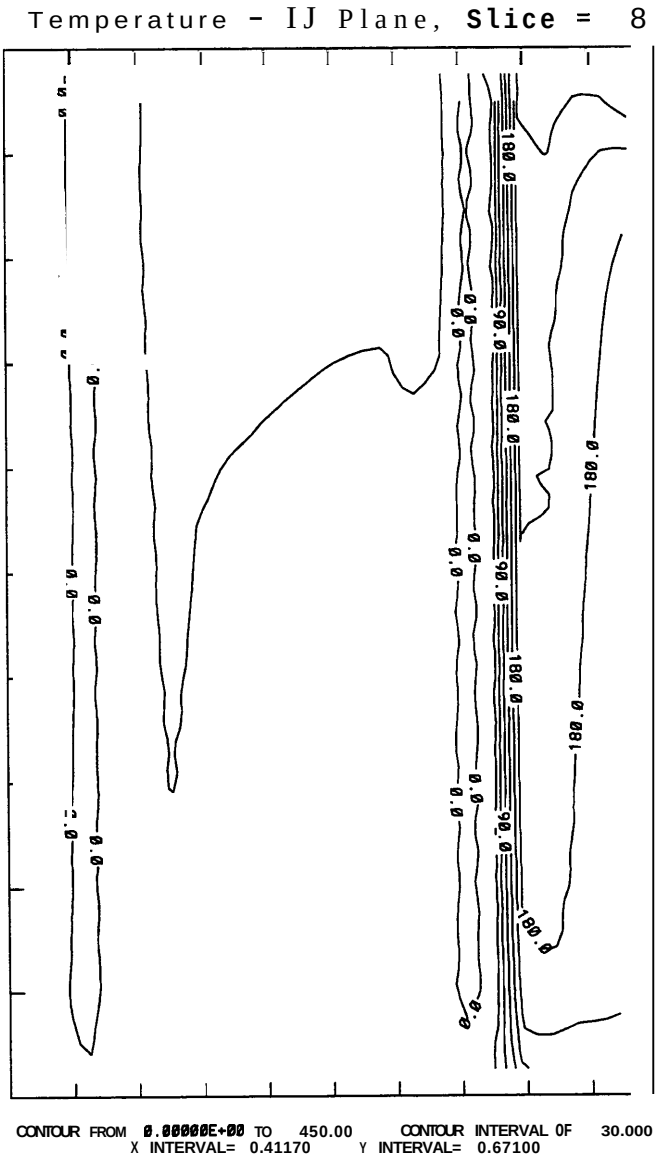


Figure 8: Numerical Temperature Rise Contours (K) for Experiment 16 - Slice 8, **A** Plane Parallel to the Floor Just Below the Ceiling

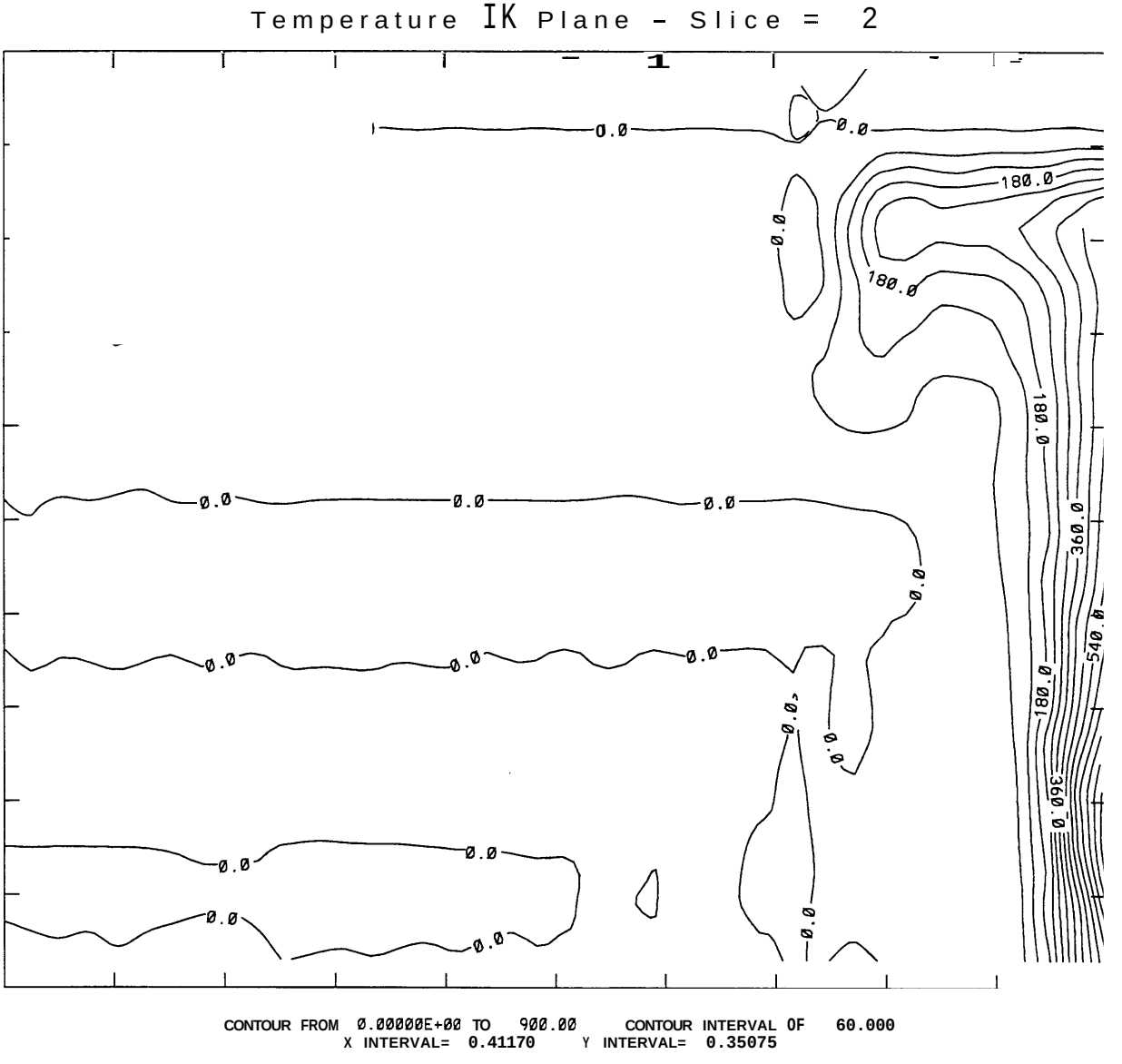


Figure 9: Numerical Temperature Rise Contours (K) for Experiment 16 - Slice 2, **A** Vertical Plane Containing the Fire, Perpendicular to the Beams

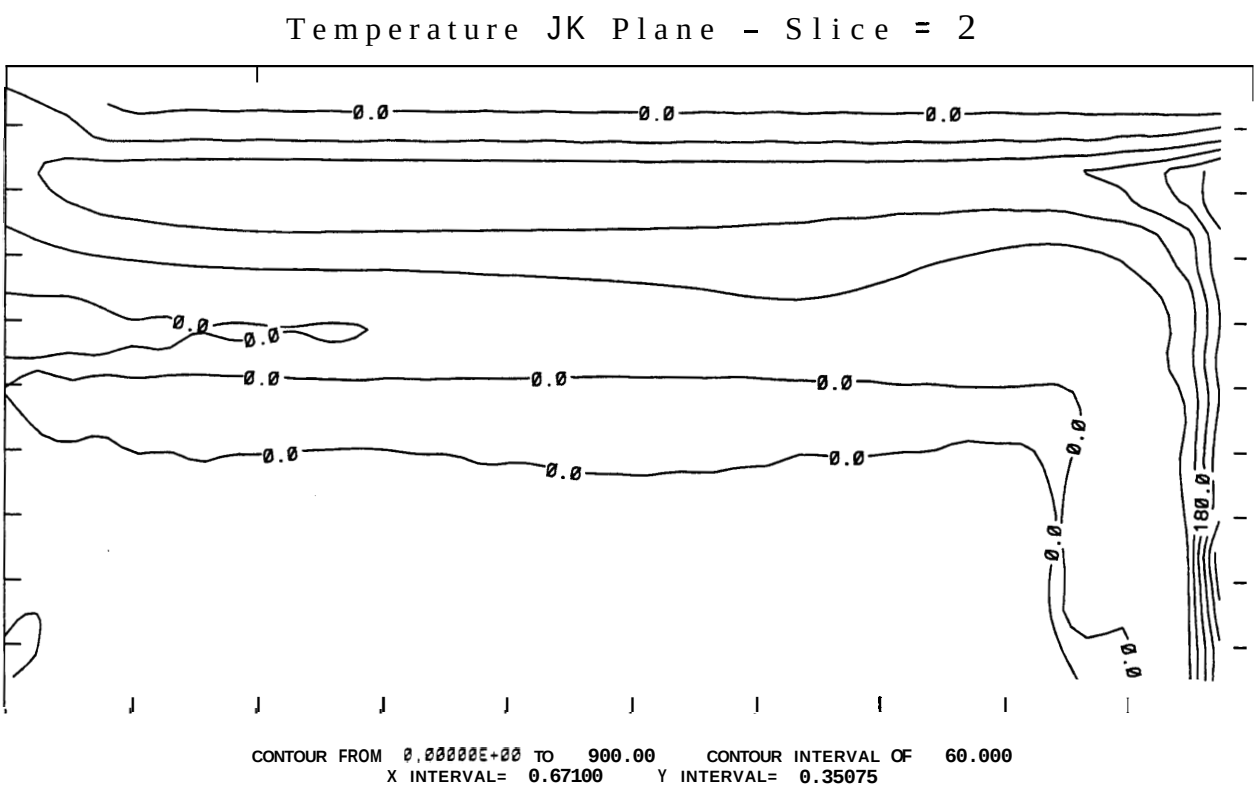


Figure 10: Numerical Temperature Rise Contours (K) for Experiment 16 - Slice 2, **A** Vertical Plane Containing the Fire Parallel to the Beams

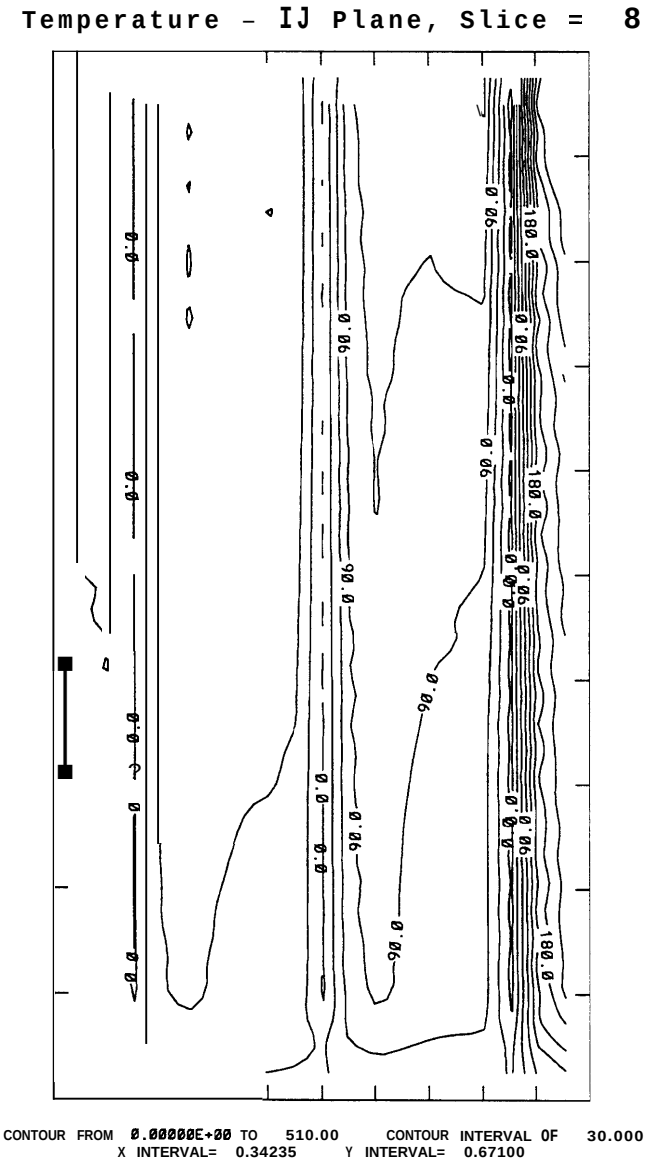


Figure 11: Numerical Temperature Rise Contours (K) For a 0.152 m (6 inch) Beam Depth Configuration. Beams are Spaced 1.22m (4 ft) Apart. The Slice is Parallel with the Floor Near the Ceiling.

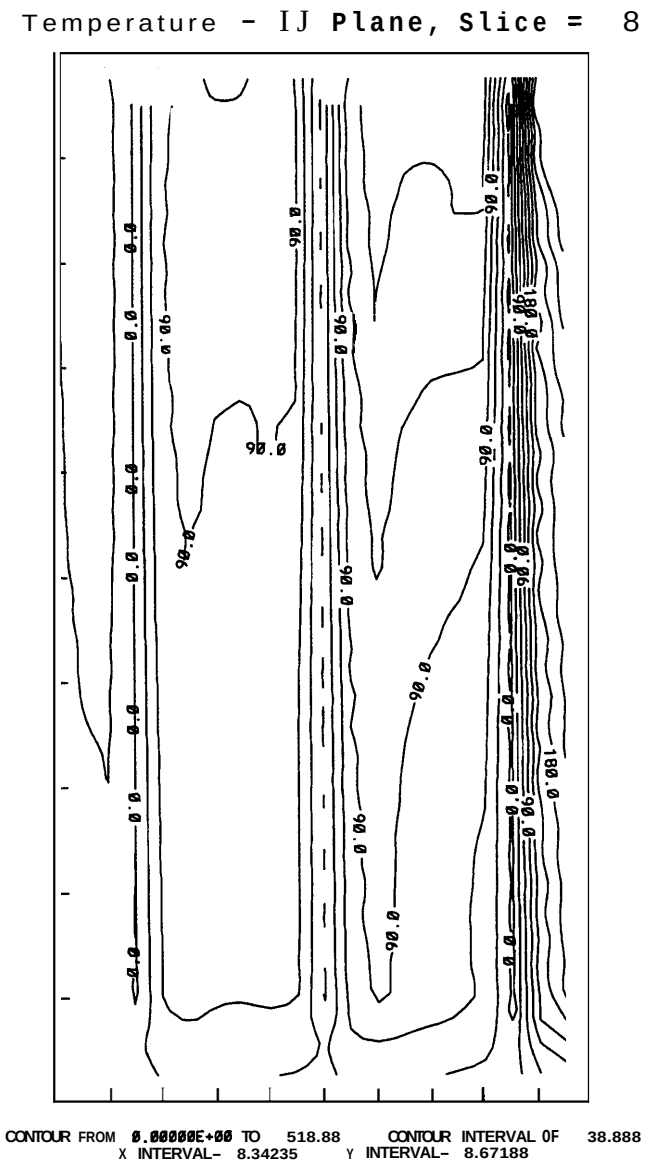


Figure 12: Numerical Temperature Rise Contours (K) For a **0.076** m **(3** inch) Beam Depth Configuration. Beams are Spaced 1.22m (4 ft) Apart. The Slice is Parallel with the Floor Near the Ceiling.

# 5 Conclusions

This work has demonstrated the ability of a numerical model to predict the temperature distribution for fire scenarios involving beamed ceilings. Two representative experiments from **[3]** were shown to be in substantial agreement with numerical predictions provided by the field model. With the field model verified for experiments of this type, further work beyond the scope of the original experiments can be performed in order to evaluate and provide a sound basis for improvements to NFPA 13 and 72E.

# References


[1] G. Heskestad and M. A. Delichatsios. Environments of Fire Detectors - Phase I: Effect of Fire Size, Ceiling Height and Material, Volume I. Measurements. Nbs-gcr-77-86, National Institute of Standards and Technology, 1977.

[2] G. Heskestad and M. A. Delichatsios. Environments of Fire Detectors - Phase I: Effect of Fire Size, Ceiling Height and Material, Volume 11. Analysis. Nbs-gcr-77-95, National Institute of Standards and Technology, 1977.

[3] G. Heskestad and M. A. Delichatsios. Environments of Fire Detectors - Phase 11: Effect of Ceiling Configuration. Volume I. Measurements. Nbs-gcr-78-128, National Institute of Standards and Technology, 1978.

[4] G. Heskestad and M. A. Delichatsios. Environments of Fire Detectors - Phase 11: Effect of Ceiling Configuration. Volume I. Analysis. Nbs-gcr-78-129, National Institute of Standards and Technology, 1978.

[5] CFD Department, AEA Industrial Technology, Harwell Laboratory, Oxfordshire, United Kingdom. *HARWELL-FLOW3D Release* **2.3:** *User Manual,* July 1990.

[6] S. Simcox, N. S. Wilkes, and I. P. Jones. Computer simulation of the flows of hot gases from the fire at king's cross underground station. In *Institution of Mechanical Engineers (IMechE) King's Cross Underground Fire: Fire Dynamics and the Organization of Safety,* pages 19–25, London, England, 1989.

[7] K. Moodie and S. F. Jagger. The technical investigation of the fire at london's king's cross underground station. *J.* of *Fire Prot. Engr.,* 3:49–63, 1991.

[8] William D. Davis, Glenn P. Forney, and John H. Klote. Field modeling of room fires. NISTIR 4673, National Institute of Standards and Technology, 1991.

[9] Glenn P. Forney and William D. Davis. Analyzing strategies for eliminating flame blow-down occuring in the navy's 19f4 fire fighting trainer. NISTIR 4825, National Institute of Standards and Technology, 1992.

[10] Roger Peyret and Thomas D. Taylor. *Computational Methods for Fluid Flow.* Springer-Verlag, New York, 1983.

[11] Ronald F. Boisvert, Sally E. Howe, David K. Kahaner, and Jeanne L. Springmann. Guide to Available Mathematical Software. NISTIR 90-4237, National Institute of Standards and Technology, 1990. **Also** available as PB90-216508/AS, National Technical Information Service, Springfield, VA 22161.

[12] Carl de Boor. *A Practical Guide to Splines.* Springer-Verlag, New York, 1978.

[13] Carl de Boor. Efficient computer manipulation of tensor products. *ACM Transactions on Mathematical Software*, **5**:173–182, 1978.